Preparation, Characterization and Electrochemical Properties of Mixed-ligand Ruthenium(III) and Ruthenium(II) Complexes with Two Kinds of β-Diketones*

YOSHIMASA HOSHINO**, YASUHIKO YUKAWA†, TETSUFUMI MARUYAMA, AKIRA ENDO, KUNIO SHIMIZU and GEN P. SATÔ††

Department of Chemistry, Faculty of Science and Technology, Sophia University, Kioicho 7-1, Chiyoda-ku, Tokyo 102 (Japan)

(Received December 12, 1989)

Abstract

The mixed-ligand ruthenium(III) complexes with the following compositions were synthesized and isolated chromatographically: $[Ru(acac)_2(tfpb)]$, $[Ru(acac)(tfpb)_2]$, $[Ru(acac)_2(hfac)]$ and $[Ru(dpm)_2(hfac)]$ ($acac^-$, 2,4-pentanedionate ion; $tfpb^-$, 4,4,4-trifluoro-1-phenyl-1,3-butanedionate ion; $hfac^-$, 1,1,1,5,5,5-hexafluoro-2,4-pentanedionate ion; dpm^-, 2,2,6,6-tetramethyl-3,5-heptanedionate ion). Attempts to isolate $[Ru(acac)(hfac)_2]$ failed; but a mixture of $K[Ru(acac)(hfac)_2]$ and $K[Ru(hfac)_3]$ was obtained. The structure of one of the three geometrical isomers of $[Ru(acac)(tfpb)_2]$ was determined by means of single-crystal X-ray structure analysis. The ^1H NMR and UV–Vis spectral data of the isolated complexes are presented. Each of these complexes gave a Nernstian one-electron reduction step and a Nernstian or quasi-Nernstian one-electron oxidation step in 0.1 mol dm^{-3} $(C_2H_5)_4NClO_4$–acetonitrile solution at 25 °C. The linear dependence of their reversible half-wave potentials on the ligand composition is discussed in detail.

Introduction

A few octahedral metal complexes with two kinds of β-diketonates have been studied [3–8]. Recently, stereoisomerism and electrochemical behavior of cobalt(III) complexes with two different β-diketonates, one of which is an unsymmetrical ligand, have been investigated in detail by Saar *et al.* [9]. The electrochemistry of mixed-ligand β-diketonato complexes of ruthenium has only been reported in one paper [10] to the authors' knowledge. The system studied there, however, was a mixture of $[Ru(acac)_2(hfac)]$ and $[Ru(acac)(hfac)_2]$, where $acac^-$ is the anion of 2,4-pentanedione and $hfac^-$ is the anion of 1,1,1,5,5,5-hexafluoro-2,4-pentanedione.

A number of tris(β-diketonato)ruthenium(III) complexes have been prepared [11–21], and their electrochemistry has often been investigated since the work of Patterson and Holm [10]. The linear dependence of the reversible half-wave potential of the oxidation steps [15, 18] and the reduction steps [16, 18] on the Hammett constants of the β- and γ-substituents of the ligands have been reported recently. The reversible half-wave potentials of the one-electron reduction steps of several tris(β-diketonato)ruthenium complexes were also linearly correlated with the first ionization energies of these molecules in the gas phase [19].

This paper describes the synthesis and characterization of some mixed-ligand β-diketonatoruthenium complexes. Their electrochemical behavior was studied in an acetonitrile system, and relationships between the ligand composition and the reversible half-wave potential of their oxidation and reduction are discussed in detail. The complexes studied here are $[Ru(dpm)_2(hfac)]$ and the members of two complete series of compounds $[Ru(acac)_n(hfac)_{3-n}]$ and $[Ru(acac)_n(tfpb)_{3-n}]$ (n = 0, 1, 2 and 3), where $tfpb^-$ is the anion of 4,4,4-trifluoro-1-phenyl-1,3-butanedione and dpm^- is the anion of 2,2,6,6-tetramethyl-3,5-heptanedione. Among them, $[Ru(tfpb)_3]$ has two geometrical isomers and $[Ru(acac)(tfpb)_2]$ has three as shown in Fig. 1. The preparation of these complexes is described in the following subsections, but the preparative method of $K[Ru(tfpb)_3]$ is given elsewhere [20] where the ligand is abbreviated as 'bhfa'.

Experimental

Preparation of the Complexes

$[Ru(acac)_n(tfpb)_{3-n}]$ series

A mixture containing all the members of this series was obtained by means of the 'ruthenium blue'

*For preliminary notes, see ref. 1a and b. Part of Doctoral Thesis of Y. Hoshino [2].

**Present address: Nihon University, College of Pharmacy, 7-7-1, Narashinodai, Funabashi-shi 274, Japan.

†Present address: General Education Department, Niigata University, 8050, Ikarashi Nino-cho, Niigata 950-21, Japan.

††Author to whom correspondence should be addressed.

0020-1693/90/$3.50

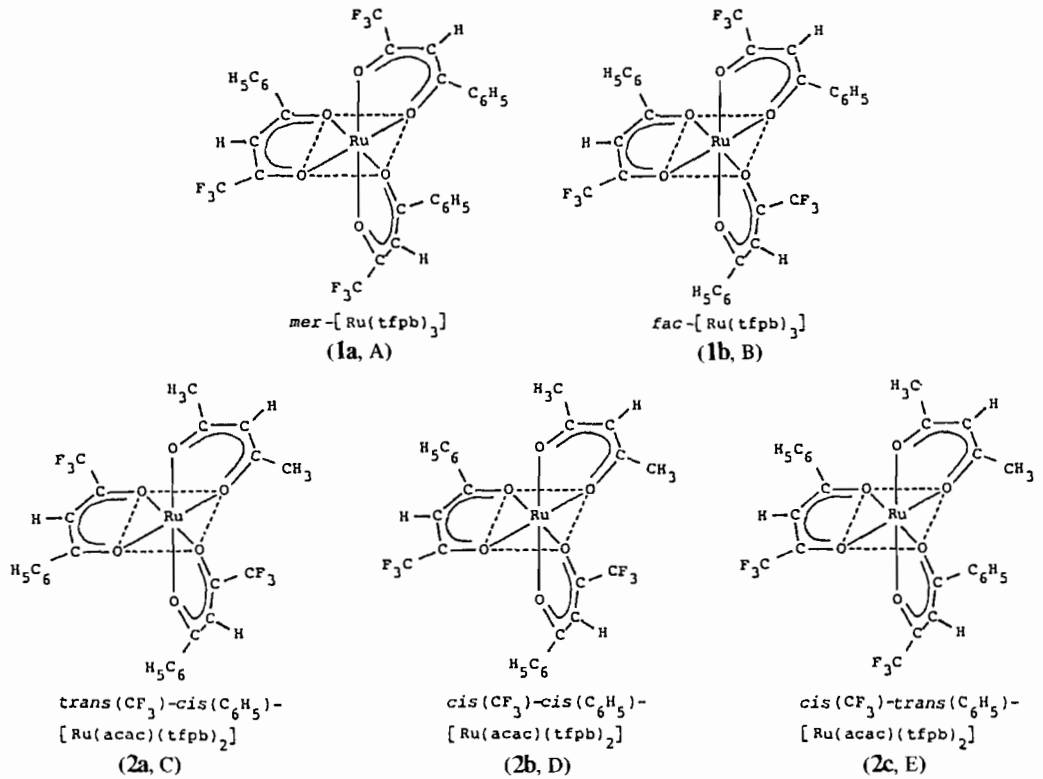

Fig. 1. Configurations of the geometrical isomers of $[Ru(tfpb)_3]$ and $[Ru(acac)(tfpb)_2]$. The capital letters correspond to the products in Fig. 2.

solution method [20, 21]. Hydrated ruthenium trichloride (1 g, 4.4 mmol as Ru) was dissolved in a mixture of water (50 cm^3) and ethanol (100 cm^3). The solution was refluxed on a steam bath for 4–5 h, when the color of the solution turned green–blue. Then Hacac (0.48 g, 4.8 mmol) and Htfpb (2.09 g, 9.68 mmol) were added to the solution at one time. The total amount-of-substance ratio of the ligands to Ru was 3.3. The mixture was refluxed until its color turned purple (for *c.* 30 min). A portion of potassium hydrogencarbonate was added after the mixture was cooled, and the mixture was refluxed again for 1 h; this procedure was repeated. The amount-of-substance ratio of $KHCO_3$ to the ligands was 1.0. The color of the mixture gradually turned purple–red. Then the solution was concentrated to *c.* 40 cm^3 in a rotary evaporator. The crude crystals deposited were collected and dried under a vacuum. Complete separation of these complexes was achieved by means of preparative thin-layer chromatography on silica gel and column chromatography according to the scheme shown in Fig. 2.

These complexes will be numbered as follows: **1a**, *mer-* and **1b**, *fac*-$[Ru(tfpb)_3]$; 2a, *ab*-acetylacetonato-*fc,de*-bis(4,4,4-trifluoro-1-phenyl-1,3-butanedionato)ruthenium(III) or *trans*(CF_3)-*cis*(C_6H_5)-$[Ru(acac)(tfpb)_2]$; **2b**, *ab*-acetylacetonato-*fc,de*-bis(4,4,4-trifluoro-1-phenyl-1,3-butanedionato)ruthenium(III) or *cis*(CF_3)-*cis*(C_6H_5)-$[Ru(acac)(tfpb)_2]$; 2c, *ab*-acetylacetonato-*cf-ed*-bis(4,4,4-trifluoro-1-phenyl-1,3-butanedionato)ruthenium(III) or *cis*(CF_3)-*trans*(C_6H_5)-$[Ru(acac)(tfpb)_2]$; 3, $[Ru(acac)_2(tfpb)]$; 4, $[Ru(acac)_3]$.

$[Ru(acac)_2(hfac)]$ (5)

A 'ruthenium blue' solution containing 4.4 mmol Ru was prepared under argon gas (anaerobic conditions improved the yield). First, 7.26 mmol of Hacac was added to the solution, and the mixture was refluxed for *c.* 30 min. After the mixture was cooled to room temperature, 0.51 g (5.1 mmol) of $KHCO_3$ was added, and the mixture was refluxed again for 30 min. Then 7.26 mmol of Hhfac was introduced, and refluxing was continued for *c.* 30 min. After another portion (9 mmol) of $KHCO_3$ was added, the mixture was refluxed again for 40 min. The color of the mixture gradually turned dark purple–red. The solution was concentrated to *c.* 30 cm^3. The precipitate was collected by filtration and dried under a vacuum. It was then extracted with benzene. The extract was concentrated to *c.* 10 cm^3 in a rotary evaporator. The dark purple–red concentrate was passed through a column of silica gel 60 (Merck) and the column was washed with benzene. The dark purple–red eluate was evaporated to dryness, and the solid was dissolved in a mixture

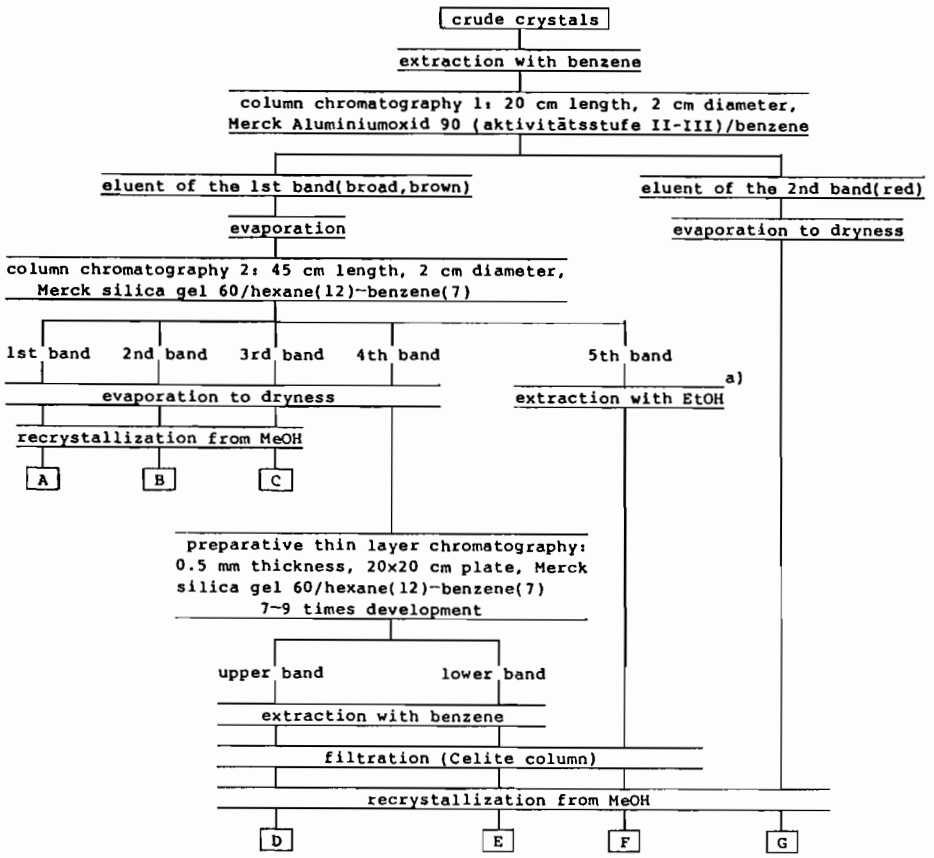

Fig. 2. Scheme for the isolation of $[Ru(acac)_n(tfpb)_{3-n}]$ series. **A**, *mer*-$[Ru(tfpb)_3]$ (**1a**); **B**, *fac*-$[Ru(tfpb)_3]$ (**1b**); **C**, *trans*(CF_3)-*cis*(C_6H_5)-$[Ru(acac)(tfpb)_2]$ (**2a**); **D**, *cis*(CF_3)-*cis*(C_6H_5)-$[Ru(acac)(tfpb)_2]$ (**2b**); **E**, *cis*(CF_3)-*trans*(C_6H_5)-$[Ru(acac)(tfpb)_2]$ (**2c**); **F**, $[Ru(acac)_2(tfpb)]$ (**3**); **G**, $[Ru(acac)_3]$ (**4**). [a]The red–brown band (5th band) was taken out of the column and extracted with ethanol.

of benzene and hexane (7:12 by volume). The solution was poured onto another column of Merck silica gel 60, and the column was washed with the same solvent. The compound obtained by evaporating the eluate to dryness was recrystallized from methanol. The dark purple–red crystals were dried under a vacuum (yield 6.6% on the basis of ruthenium trichloride).

K[Ru(acac)(hfac)$_2$] (6)

A number of attempts at complete isolation of this complex failed, and only a relatively pure sample contaminated by $K[Ru(hfac)_3]$ was obtained by the following procedure. A 'ruthenium blue' solution was prepared from 1.5 mmol Ru under argon. The solution was cooled to 0 °C and Hacac (0.28 g, 2.8 mmol) and Hhfac (0.50 g, 2.4 mmol) were added at one time together with $KHCO_3$ (0.48 g, 4.8 mmol), and the mixture was warmed up to *c.* 30 °C at a heating rate of 0.75 °C min^{-1}. The color of the solution gradually turned purple–brown. Then the mixture was cooled again to *c.* 0 °C. The precipitate which appeared at this stage was filtered off, and the filtrate was poured onto a column of Sephadex LH-20 (3.5 cm internal diameter, 46 cm long). The column was eluted with ethanol. The second-band eluate (brown–red) was collected and concentrated to *c.* 10 cm^3 quickly in a rotary evaporator, when some precipitate was formed. The precipitate was filtered off. The filtrate, which contained K[Ru(acac)(hfac)$_2$], was subjected to flush column chromatography on silica gel 60 (3.5 cm internal diameter, 40 cm long). 2-Methyl-2-propanol was used as the developing agent to minimize decomposition. Fractions of the purple–red eluate were collected. Some part of the complex in these fractions was in the ruthenium(III) state. It was reduced back to the ruthenium(II) state by the addition of a slight excess of $K[Ru(tfpb)_3]$ (this reductant was chosen because it was soluble in propanol and its oxidation form was readily extracted into benzene). The mixture was evaporated to dryness and the solid was treated with benzene in order to extract the ruthenium(III) species. The residue was collected by filtration and dried under a vacuum. It still contained an appreciable amount of $K[Ru(hfac)_3]$.

[Ru(dpm)$_2$(hfac)] (7)

A procedure similar to that for [Ru(acac)$_2$(hfac)] was used. The amount-of-substance ratio of Hdpm to Ru was 2.3, and that of Hhfac to Ru was 1.7. The crude crystals were dissolved in benzene and the insoluble residue was filtered off. The purple–red solution was evaporated to dryness. The solid was dissolved in a small volume of benzene–hexane mixture (1:3 by volume) and the solution was subjected to column chromatography (silica gel 60, 2 cm diameter, 36 cm long). Development with the benzene–hexane mixture gave rise to two zones. The eluate of the second zone, which was dark purple–red, was concentrated to *c.* 2 cm^3. The solution was poured onto a column of silica gel (2 cm diameter, 37 cm long) and washed with a mixture of benzene–hexane (volume ratio, 1:5). The dark purple–red eluate was evaporated to dryness. The solid was recrystallized from methanol–water and the crystals were dried under a vacuum. The yield was 1.4%.

Other Chemicals

Tetraethylammonium perchlorate (TEAP) of special polarographic grade and hydrated ruthenium trichloride were obtained from Nakarai Chemical Ltd. High purity acetonitrile for spectrometry (Dotite Spectrosol) was used for the measurement of UV–Vis spectra, but acetonitrile for electrochemical experiments was purified as described previously [18]. Chromatographic grade benzene and hexane were used throughout. The β-diketones were purchased from Dojindo Laboratories. Deuterated chloroform was purchased from C.E.A., France.

Single Crystal X-ray Structure Analysis of trans(CF$_3$)-cis(C$_6$H$_5$)-[Ru(acac)(tfpb)$_2$] (2a)

About 30 mg of product **C** (Fig. 2) was dissolved in ethanol (*c.* 80 cm^3), and the solution was concentrated to *c.* 5 cm^3 on a steam bath. The nearly saturated solution, after being cooled to room temperature, was allowed to stand still in a closed vessel containing water. After a week, deep brown–red, plate crystals were obtained. Several suitable crystals were selected for the X-ray structure analysis.

The Laue symmetry and approximate cell dimensions were determined from Weissenberg photographs taken with Cu Kα radiation. The cell dimensions were refined by the least-squares analysis of the θ values of 25 reflections measured on a Rigaku AFC-6A automated four-circle diffractometer with Mo Kα radiation. Crystal data: orthorhombic, with space group *Pbca*, a = 17.970(6), b = 18.296(3), c = 15.762(3) Å, (Å = 10^{-10} m), V = 5182(2) Å^3, μ(Mo Kα) = 6.58 cm^{-1}, M_r = 630.5, Z = 8, D_m (flotation) = 1.59 g cm^{-3}, D_x = 1.62 g cm^{-3}.

Intensity data were collected by using the diffractometer operating in the ω–2θ scan mode with graphite-monochromated Mo Kα radiation (0.7107 Å). A crystal specimen of 0.18 × 0.40 × 0.08 mm was used. Structure refinement was carried out by using 2314 independent reflections with $|F_o| > 3\sigma(|F_o|)$. The intensities were corrected for Lorentz and polarization factors, but no correction was made for the absorption. All calculations were carried out on HITAC M-200H and HITAC M-680H computers at the Computer Center of the University of Tokyo by using a local version of UNICS [22]. The atomic scattering factors were taken from the published tables [23].

The position of the Ru atom was obtained from a three-dimensional Patterson function, while the positions of all the non-hydrogen atoms were successively located by the Fourier syntheses. The hydrogen atoms (except for the CH_3 group) were placed into the calculated positions with a fixed value of C–H 1.08 Å. The positional, isotropic and then anisotropic parameters of the non-hydrogen atoms (except for CF_3 groups) were refined by a repeated block-diagonal least-squares method. The weighting scheme was $w = 1/[\{\sigma(|F_o|)\}^2 + (0.025 \times |F_o|)^2]$. The final R value ($R = \{\Sigma||F_o| - |F_c||\}/\Sigma|F_o|$) was 0.098.

Measurements

The ^{1}H NMR spectra of the complexes in $CDCl_3$ at room temperature were obtained on JEOL JNM FX-200 and GX-270 instruments. A Hitachi Model 200-20 spectrophotometer was used for recording UV–Vis spectra.

Voltammograms of the complexes in acetonitrile containing 0.1 mol dm^{-3} TEAP at (25 ± 0.1) °C were recorded with a stationary platinum disk electrode (SPtDE, ϕ = 1.99 mm) as described previously [18]. All the potentials were measured against a silver–silver ion reference electrode, Ag/0.1 mol dm^{-3} $AgClO_4$–acetonitrile.

Results and Discussion

Syntheses and Ligand Exchange Reactions

The elemental analyses of [Ru(acac)$_n$(tfpb)$_{3-n}$] (n = 0, 1 and 2), [Ru(acac)$_2$(hfac)] and [Ru(dpm)$_2$(hfac)] are presented in Table 1. The total yield of [Ru(acac)(tfpb)$_2$] and [Ru(acac)$_2$(tfpb)] was 20.1% based on hydrated ruthenium trichloride. The yield was 6.6% for [Ru(acac)$_2$(hfac)] and 1.4% for [Ru(dpm)$_2$(hfac)]. The yields of the mixed-ligand complexes tended to decrease when the reversible half-wave potentials for the Ru^{III}/Ru^{II} process of the end members were widely separated.

An alternative preparative method for mixed-ligand β-diketonatoruthenium complexes, which is based on the substitution of bis(acetonitrile)bis(acetylacetonato)ruthenium(II), has been published recently [24]. This method is suitable when mixed-

TABLE 1. Elemental analyses[a]

Complex	Ru (%)	C (%)	H (%)
mer-[Ru(tfpb)$_3$] (**1a**)	13.1(13.5)	48.25(48.27)	2.29(2.43)
fac-[Ru(tfpb)$_3$] (**1b**)	(13.5)	48.52(48.27)	2.59(2.43)
trans-(CF_3)-*cis*(C_6H_5)-[Ru(acac)(tfpb)$_2$] (**2a**)	16.0(16.0)	47.34(47.63)	2.97(3.04)
cis-(CF_3)-*cis*(C_6H_5)-[Ru(acac)(tfpb)$_2$] (**2b**)	(16.0)	47.66(47.63)	3.04(3.04)
cis-(CF_3)-*trans*(C_6H_5)-[Ru(acac)(tfpb)$_2$] (**2c**)	(16.0)	47.57(47.63)	3.05(3.04)
[Ru(acac)$_2$(tfpb)] (**3**)	19.9(19.6)	46.42(46.70)	3.86(3.92)
[Ru(acac)$_2$(hfac)] (**5**)	20.0(20.0)	35.30(35.58)	2.89(2.99)
[Ru(dpm)$_2$(hfac)] (**7**)	(15.0)	47.87(48.07)	5.70(5.83)

[a]Calculated values are given in parentheses.

ligand complexes of the type [Ru(acac)$_2$L] are to be prepared. The present method, on the other hand, is more useful for the syntheses of a series of mixed-ligand complexes at one step.

Labile equilibria, however, presented difficulty. When a 'ruthenium blue' solution was treated with Hacac and Hhfac, $[Ru^{II}(acac)(hfac)_2]^-$ was formed at an early stage. But it underwent substitution reactions with the ligands still present in excess (Scheme 1), and it no longer remained when the reaction was completed. Even by careful adjustment of the reaction conditions as described before, only a mixture of $K[Ru^{II}(acac)(hfac)_2]$ and $K[Ru^{II}(hfac)_3]$ was obtained. Attempts to isolate the former by means of chromatography were so far unsuccessful.

$$[Ru^{II}(acac)(hfac)_2]^- \begin{cases} + \text{Hacac} \longrightarrow [Ru^{II}(acac)_2(hfac)]^- \\ + \text{Hhfac} \longrightarrow [Ru^{II}(hfac)_3]^- \end{cases}$$

Scheme 1.

The following observation indicates the presence of such ligand exchange reactions. When Hhfac was added to an ethanolic solution of the mixture of $K[Ru^{II}(acac)(hfac)_2]$ and $K[Ru^{II}(hfac)_3]$ at room temperature, the visible absorption spectrum began to change slowly. The absorption band at 370 nm intensified at the expense of the absorption bands at 490 and 528 nm, and the shoulder at 570 nm disappeared after 4 h. There was an isosbestic point at 442 nm. The spectrum finally became the same as that of $K[Ru^{II}(hfac)_3]$.

The failure to isolate K[Ru(dpm)(hfac)$_2$] can be attributed to similar ligand-exchange reactions.

Identification of Geometrical Isomers

Product **A**, **B** and **D** in Fig. 1 were identified on the basis of the ^{1}H NMR data. Product **A** showed three signals from the methine protons of the tfpb$^-$ ligands, whereas product **B** showed only one signal. Accordingly, product **A** is *mer*-[Ru(tfpb)$_3$], which has no symmetry, and product **B** is *fac*-[Ru(tfpb)$_3$], which has C_3 symmetry. Product **D** gave rise to eleven signals, and product **C** and **E** six each (Table 2). Therefore, product **D** is identified as *cis*(CF_3)-*cis*(C_6H_5)-[Ru(acac)(tfpb)$_2$], which has no symmetry.

Discrimination between *trans*(CF_3)-*cis*(C_6H_5)-[Ru(acac)(tfpb)$_2$] and *cis*(CF_3)-*trans*(C_6H_5-[Ru(acac)(tfpb)$_2$] is not possible from the NMR spectra, since both have C_2 symmetry. The X-ray analysis of product **C** revealed that this was *trans*(CF_3)-*cis*(C_6H_5)-[Ru(acac)(tfpb)$_2$] (Fig. 3; details are presented in a later section). Then product **E** must be *cis*(CF_3)-*trans*(C_6H_5)-[Ru(acac)(tfpb)$_2$].

^{1}H NMR Spectroscopy

Table 2 presents the ^{1}H NMR data of the complexes in $CDCl_3$ at ambient temperature together with the assignment of the signals. The NMR spectra exhibit paramagnetic shifts. The assignment of the methine, methyl and t-butyl signals in the mixed-ligand complexes with C_2 symmetry (*trans*(CF_3)-*cis*(C_6H_5)-[Ru(acac)(tfpb)$_2$], *cis*(CF_3)-*trans*(C_6H_5)-[Ru(acac)(tfpb)$_2$], [Ru(acac)$_2$(hfac)] and [Ru(dpm)$_2$(hfac)]) was based on the integral ratios and on the comparison with the spectra of [Ru(acac)$_3$] and [Ru(dpm)$_3$] [20, 25, 26]. Complete assignment of the methine signals in the complexes with no symmetry (*mer*-[Ru(tfpb)$_3$], *cis*(CF_3)-*cis*(C_6H_5)-[Ru(acac)(tfpb)$_2$] and [Ru(acac)$_2$(tfpb)]) was not possible owing to the lack of information about the unpaired-electron spin densities of the individual chelate rings in these complexes. The phenyl protons were assigned on the basis of both the integral ratios and the paramagnetic shift pattern of the π ring system in the phenyl group: the *o*-H and the *p*-H shift to the same direction, whereas the *m*-H shifts to the opposite field [27–29].

The paramagnetic shifts in tris(β-diketonato)-ruthenium(III) complexes can arise from both the contact interaction and the pseudo-contact interaction [25]. All the methine proton signals are shifted upfield from the corresponding signals of the diamagnetic tris(β-diketonato)metal complexes [3, 30, 31], and their half-peak widths are large, *c.* 100–200 Hz. It is noted that the methine proton signal of the acac$^-$ ring of *trans*(CF_3)-*cis*(C_6H_5)-

TABLE 2. ^1H NMR data in $CDCl_3$

Complex	Ligand	δ (ppm)		
		CH_3	CH	Others $\{C_6H_5, C(CH_3)_3\}$
mer-[Ru(tfpb)$_3$] (**1a**)	tfpb$^-$		−21.7, −41.5, −49.7	10.9, 10.9, 11.5 (*o*) 6.3, 7.2, 6.0 (*m*) 9.0, 8.4, 9.5 (*p*)
fac-[Ru(tfpb)$_3$] (**1b**)	tfpb$^-$		−35.5	11.7 (*o*) 6.9 (*m*) 9.0 (*p*)
trans(CF_3)-*cis*(C_6H_5)-[Ru(acac)(tfpb)$_2$] (**2a**)	acac$^-$ tfpb$^-$	−12.4	−51.2 −28.8	 11.0 (*o*) 6.7 (*m*) 8.6 (*p*)
cis(CF_3)-*cis*(C_6H_5)-[Ru(acac)(tfpb)$_2$] (**2b**)	acac$^-$ tfpb$^-$	−8.0, −8.5	−27.1, −39.8, −41.3	 11.2, 11.3 (*o*) 7.0, 6.3 (*m*) 8.6, 9.3 (*p*)
cis(CF_3)-*trans*(C_6H_5)-[Ru(acac)(tfpb)$_2$] (**2c**)	acac$^-$ tfpb$^-$	−3.8	−25.0 −42.6	 10.8 (*o*) 6.2 (*m*) 9.3 (*p*)
[Ru(acac)$_2$(tfpb)] (**3**)	acac$^-$ tfpb$^-$	−2.1, −3.8, −7.3, −8.4	−24.4, −36.3, −37.3	 11.6 (*o*) 6.5 (*m*) 9.4 (*p*)
[Ru(acac)$_3$][a] (**4**)	acac$^-$	−5.5	−29.9	
[Ru(acac)$_2$(hfac)] (**5**)	acac$^-$ hfac$^-$	−6.3, −7.9	−36.1 −35.1	
[Ru(dpm)$_2$(hfac)] (**7**)	dpm$^-$ hfac$^-$		−50.4 −19.6	1.9, 3.5
[Ru(dpm)$_3$][a] (**8**)	dpm$^-$		−32.8	2.53

[a]From ref. 20.

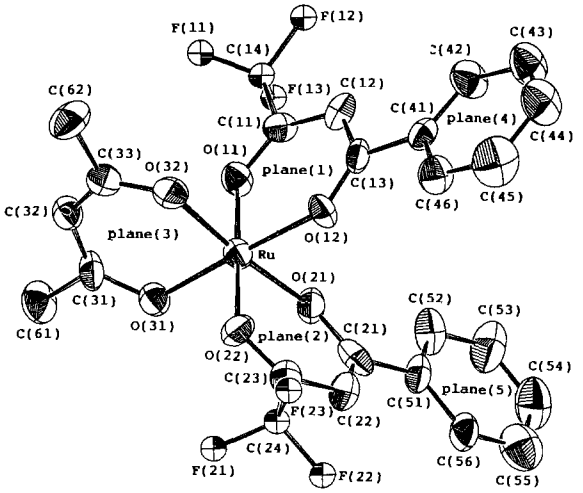

Fig. 3. Perspective drawing of product C (*trans*(CF_3)-*cis*-(C_6H_5)-[Ru(acac)(tfpb)$_2$]) with the numbering scheme of the atoms.

[Ru(acac)(tfpb)$_2$] is more upfield than the methine protons signals of the tfpb$^-$ ring, and the reverse is true for *cis*-(CF_3)-*trans*(C_6H_5)-[Ru(acac)(tfpb)$_2$]. This fact indicates that the paramagnetic shift of the methine protons is predominantly caused by the contact interaction, because the methine proton signals of both the acac$^-$ ring and the tfpb$^-$ ring would be shifted to the same direction and to the same extent if the pseudo-contact interaction were predominant.

X-ray Structure of trans(CF_3)-cis(C_6H_5)-[Ru(acac)(tfpb)$_2$]

The molecular structure is shown in Fig. 3 with the numbering scheme of the atoms. Selected interatomic distances and angles are given in Table 3. The average Ru–O bond length in the acac$^-$ chelate ring agrees well with the reported values (2.00 Å) [32, 33]. There are two kinds of Ru–O bond lengths in the tfpb$^-$ rings, i.e. the Ru–O bonds nearest to

TABLE 3. Selected bond lengths and angles of *trans*(CF_3)-*cis*(C_6H_5)-[Ru(acac)(tfpb)$_2$] with standard deviations

Bond lengths (Å)					
Ru–O(11)	1.98(1)	Ru–O(21)	1.98(1)	Ru–O(31)	2.01(1)
Ru–O(12)	2.01(1)	Ru–O(22)	1.99(1)	Ru–O(32)	1.99(1)
O(11)–C(11)	1.23(2)	O(21)–C(21)	1.32(2)	O(31)–C(31)	1.25(2)
O(12)–C(13)	1.26(2)	O(22)–C(23)	1.24(2)	O(32)–C(33)	1.29(2)
C(11)–C(12)	1.41(2)	C(21)–C(22)	1.41(3)	C(31)–C(32)	1.37(2)
C(12)–C(13)	1.42(3)	C(22)–C(23)	1.41(3)	C(32)–C(33)	1.34(2)
C(11)–C(14)	1.53(3)	C(21)–C(51)	1.46(2)	C(31)–C(61)	1.55(3)
C(13)–C(41)	1.52(2)	C(23)–C(24)	1.52(3)	C(33)–C(62)	1.52(3)
C(14)–F(11)	1.22(3)	C(24)–F(21)	1.28(3)		
C(14)–F(12)	1.33(3)	C(24)–F(22)	1.32(3)		
C(14)–F(13)	1.18(4)	C(24)–F(23)	1.17(3)		
Bond angles (°)					
O(11)–Ru–O(12)	94.7(4)	O(21)–Ru–O(22)	92.1(4)		
Ru–O(11)–C(11)	122(1)	Ru–O(21)–C(21)	125(1)		
Ru–O(12)–C(13)	123(1)	Ru–O(22)–C(23)	124(1)		
O(11)–C(11)–C(12)	130(2)	O(21)–C(21)–C(22)	122(2)		
O(12)–C(13)–C(12)	126(2)	O(22)–C(23)–C(22)	128(2)		
C(11)–C(12)–C(13)	124(1)	C(21)–C(22)–C(23)	126(2)		
O(11)–C(11)–C(14)	111(2)	O(21)–C(21)–C(51)	117(2)		
C(12)–C(11)–C(14)	119(2)	C(22)–C(21)–C(51)	122(2)		
O(12)–C(13)–C(41)	116(1)	O(22)–C(23)–C(24)	112(2)		
C(12)–C(13)–C(41)	118(1)	C(22)–C(23)–C(24)	120(2)		
O(31)–Ru–O(32)	91.1(4)				
Ru–O(31)–C(31)	122.6(9)				
Ru–O(32)–C(33)	124(1)				
O(31)–C(31)–C(32)	125(2)				
O(32)–C(33)–C(32)	124(2)				
O(31)–C(32)–C(33)	129(2)				
O(31)–C(31)–C(61)	116(2)				
C(32)–C(31)–C(61)	119(1)				
O(32)–C(33)–C(62)	112(2)				
C(32)–C(33)–C(62)	125(2)				

$-CF_3$ and the Ru–O bonds nearest to C_6H_5. One pair of Ru–O bonds (Ru–O(21) and Ru–O(22)) is almost the same, but the other pair (Ru–O(11) and Ru- O(12)) is not very similar as has been found in other metal chelates with the $tfpb^-$ ligand [34, 35].

The phenyl groups were placed at 6–7° to the chelate plane, and the bond lengths, C(13)–C(41) and C(21)–C(51), were slightly longer than the $C(sp^2)$–$C(sp^2)$ bond length.

UV–Vis Spectra

The UV–Vis spectral data of the complexes in acetonitrile are presented in Table 4. The UV–Vis spectra of some tris(β-diketonato)ruthenium(III) complexes have been assigned recently [26, 36]. According to Kobayashi *et al.* [26], the three absorption bands of $[Ru(acac)_3]$ observed in the range of (18–40) × 10^3 cm^{-1} are ascribed to the excited states which are the configuration–interaction admixtures of the ligand-to-metal charge-transfer excited states and the ligand (π, π^*) excited triplets and singlets. The electronic spectra of mixed-ligand β-diketonatoruthenium(III) complexes are more difficult to assign than those of the tris complexes. The bands at *c.* 300 nm of $[Ru(acac)_n(tfpb)_{3-n}]$ (n = 0, 1 and 2), however, can be attributed to the (π, π^*) transition of the phenyl group, because no corresponding band was present in the other complexes and the intensity increased with the number of the $tfpb^-$ ligand.

Electrochemistry

The voltammetric characteristics of the mixed-ligand and tris complexes are presented in Table 5.

Each mixed-ligand complex, except $K[Ru(acac)(hfac)_2]$, showed an oxidation step and a reduction step in 0.1 mol dm^{-3} TEAP–acetonitrile on a Pt

TABLE 4. Absorption spectral data in acetonitrile

Complex	λ_{max} (nm) (log ϵ (mol^{-1} dm^3 cm^{-1}))
mer-$[Ru(tfpb)_3]$ (**1a**)	550(sh), 396(4.28), 305(4.64), 266(sh)
fac-$[Ru(tfpb)_3]$ (**1b**)	549(sh), 395(4.14), 304(4.60), 265(sh)
trans(CF_3)-*cis*(C_6H_5)-$[Ru(acac)(tfpb)_2]$ (**2a**)	536(sh), 381(4.03), 303(4.50), 260(4.30)
cis(CF_3)-*cis*(C_6H_5)-$[Ru(acac)(tfpb)_2]$ (**2b**)	540(sh), 387(3.96), 303(4.46), 261(4.25)
cis(CF_3)-*trans*(C_6H_5)-$[Ru(acac)(tfpb)_2]$ (**2c**)	550(sh), 400(4.06), 306(4.49), 262(4.27)
$[Ru(acac)_2(tfpb)]$ (**3**)	490(3.47), 380(sh), 294(4.30), 268(4.26)
$[Ru(acac)_3]$[a] (**4**)	506(3.19), 349(3.94), 272(4.24)
$[Ru(acac)_2(hfac)]$ (**5**)	505(3.31), 370(sh), 332(3.78), 283(4.13)
$[Ru(dpm)_2(hfac)]$ (**7**)	526(3.45), 338(3.82), 287(4.22)
$K[Ru(hfac)_3]$[a] (**9**)	529(4.22), 494(sh), 288(4.31), 234(3.98)

[a]From ref. 20.

TABLE 5. The reversible half-wave potentials ($E^r_{1/2}$) in 0.1 mol dm^{-3} TEAP–acetonitrile at 25 °C[a]

Complex	Ru^{IV}/Ru^{III}			Ru^{III}/Ru^{II}		
	$E^r_{1/2}$ (V)[b]	Slope (mV)[c]	ΔE_p (mV)[d]	$E^r_{1/2}$ (V)[b]	Slope (mV)[c]	ΔE_p (mV)[d]
mer-$[Ru(tfpb)_3]$ (**1a**)	1.280	[e]	110	−0.337	−25.8	67
trans(CF_3)-*cis*(C_6H_5)-$[Ru(acac)(tfpb)_2]$ (**2a**)	1.058	25.5	71	−0.577	−25.8	65
cis(CF_3)-*cis*(C_6H_5)-$[Ru(acac)(tfpb)_2]$ (**2b**)	1.055	25.8	78	−0.586	−26.0	70
cis(CF_3)-*trans*(C_6H_5)-$[Ru(acac)(tfpb)_2]$ (**2c**)	1.054	25.8	90	−0.586	−26.0	64
$[Ru(acac)_2(tfpb)]$ (**3**)	0.838	27.7	61	−0.847	−26.9	65
$[Ru(acac)_3]$ (**4**)	0.633	25.8	61	−1.138	−29.6	68
$[Ru(acac)_2(hfac)]$ (**5**)	1.047	25.1	70	−0.605	−26.0	66
$K[Ru(acac)(hfac)_2]$ (**6**)				−0.14[f]		79
$[Ru(dpm)_2(hfac)]$ (**7**)	0.910[g]	[e]	125	−0.763[g]	[e]	89
$[Ru(dpm)_3]$	0.457	26.0	59	−1.440[g]	[e]	80
$K[Ru(hfac)_3]$ (**9**)	(1.845)[h]			0.358	−27.7	68

[a]The values for **1**, **3**, **4**, **5**, **8** and **9** previously published [18] are refined or corrected. [b]Against Ag|0.1 mol dm^{-3} $AgClO_4$–acetonitrile. [c]Reciprocal slope of natural logarithmic plot. [d]Cyclic voltammetric peak separation at 0.1 V s^{-1}. [e]Quasi-Nernstian. [f]Estimated from the peak potential of the differential pulse voltammogram of a mixture of $K[Ru(acac)(hfac)_2]$ and $K[Ru(hfac)_3]$. [g]The average of the cathodic and anodic peak potentials of the cyclic voltammograms. [h]Estimated from Fig. 4.

electrode at 25 °C. The cyclic voltammogram of $K[Ru(acac)(hfac)_2]$ showed only a one-electron oxidation step. Its half-wave potential was estimated from the peak potential of the differential pulse voltammogram. No reduction step of this complex was observed within the potential window of the medium.

The analysis of the normal pulse voltammograms and the corresponding cyclic voltammograms indicated that the oxidation and the reduction steps of $[Ru(acac)_3]$, $[Ru(acac)_2(hfac)]$, $[Ru(acac)_2(tfpb)]$ and the three isomers of $[Ru(acac)(tfpb)_2]$ were Nernstian. The reduction step of *mer*-$[Ru(tfpb)_3]$ and the oxidation step of $K[Ru(acac)(hfac)_2]$ were Nernstian, too. However, the oxidation step of *mer*-$[Ru(tfpb)_3]$ and $[Ru(dpm)_2(hfac)]$ and the reduction step of $[Ru(dpm)_2(hfac)]$ were quasi-Nernstian as indicated by the dependence of the voltammetric anodic and the cathodic peak potentials on the sweep rate and the separation between them.

The controlled potential coulometry of $[Ru(acac)_2(tfpb)]$ and $[Ru(acac)_2(hfac)]$ in the acetonitrile medium confirmed that their reduction steps were of the one-electron process to the corresponding ruthenium(II) species and that the ruthenium(II) complexes were stable and electrolytically reoxidizable to the original ruthenium(III) species quantitatively. The oxidation process, on the other hand, was accompanied by slow subsequent reactions. When $[Ru^{III}(acac)_2(tfpb)]$ was electrolyzed at +1.10 V, the diffusion controlled reduction step of $[Ru^{IV}(acac)_2(tfpb)]^+$ appeared, but its diffusion current deacreased slowly when the electrolysis was suspended. In the case of the oxidation of $[Ru^{III}(acac)_2(hfac)]$, no reduction step of $[Ru^{IV}(acac)_2(hfac)]^+$ was observed, indicating the presence of relatively fast reaction(s) through which the ruthenium(IV) species was converted to some electroinactive species.

The reversible half-wave potential for the reduction of *trans*(CF_3)-*cis*(C_6H_5)-$[Ru(acac)(tfpb)_2]$ is more positive than those of *cis*(CF_3)-*cis*(C_6H_5)-$[Ru(acac)(tfpb)_2]$ and *cis*(CF_3)-*trans*(C_6H_5)-$[Ru(acac)(tfpb)_2]$, the difference being beyond the experimental uncertainty of *c.* ±3 mV. The cause of this potential shift of *trans*(CF_3)-*cis*(C_6H_5)-$[Ru(acac)(tfpb)_2]$ is not yet clear. To our knowledge, this is the first instance where such geometrical isomers (i.e. isomers with the same ligating atoms but with different positions of substituents on the ligands) show an observable difference in reversible half-wave potential.

As is shown in Fig. 4, good linear relationships exist between the ligand composition and the reversible half-wave potentials ($E^r_{1/2}$) of the oxidation and the reduction steps. In both the oxidation and reduction processes of tris(β-diketonato)ruthenium

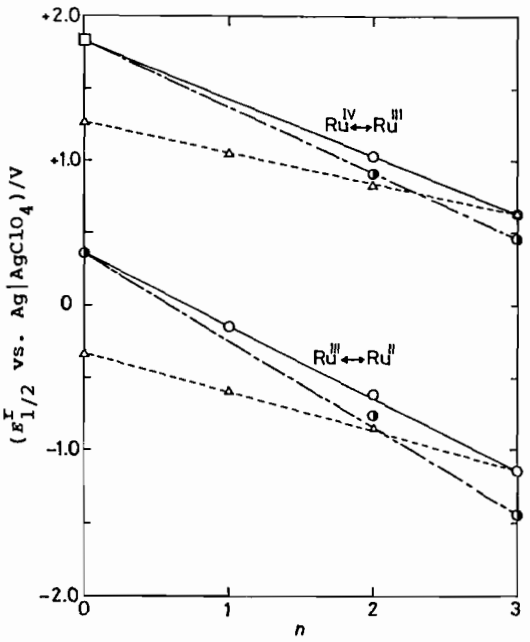

Fig. 4. Relationships between the ligand composition and the reversible half-wave potentials of β-diketonato ruthenium complexes: $[Ru(acac)_n(hfac)_{3-n}]$ (○–○); $[Ru(acac)_n(tfpb)_{3-n}]$ (△–△); $[Ru(dpm)_n(hfac)_{3-n}]$ (◑–◑); estimated value (□). Reference electrode, Ag/0.1 mol dm^{-3} $AgClO_4$–acetonitrile; 25 °C.

complexes, the electron is added to or subtracted from the dπ molecular orbital which originates from the t_{2g} orbital of ruthenium [15, 19, 40]. This holds in the mixed-ligand β-diketonato complexes, too, as indicated by the fact that the two lines of each series are almost parallel. The $E^r_{1/2}(Ru^{IV}/Ru^{III})$ value for $K[Ru(hfac)_3]$ can be estimated on the basis of this linear relationship. The estimated value (1.845 V) agrees with the extrapolated value from the linear relationship established between $E^r_{1/2}$ and the sum of the Hammett constants of the substituents on the ligands [15, 18].

According to the above linear relationships, the reversible half-wave potential of the reduction step of a mixed-ligand complex $[Ru^{III}L''_nL'_{3-n}]$ is given by

$$E_{III/II}(L''_nL'_{3-n}) = (n/3)E_{III/II}(L''_3) + (1 - n/3)E_{III/II}(L'_3) \quad (1)$$

Here $E_{III/II}(L''_3)$ is the reversible half-wave potential of the reduction step of $[Ru^{III}L''_3]$, and $E_{III/II}(L'_3)$ is that of $[Ru^{III}L'_3]$. The right-hand side of eqn. (1) can be rewritten in terms of the relative half-wave potentials of the tris complexes measured against the half-wave potential of a third tris complex $[Ru^{III}L_3]$ chosen as the reference, i.e.

$$E_{III/II}(L''_nL'_{3-n}) = n\Delta E_{III/II}(L'') + (3 - n)\Delta E_{III/II}(L') + E_{III/II}(L_3) \quad (2)$$

with

$$\Delta E_{III/II}(L'') = (1/3)\{E_{III/II}(L''_3) - E_{III/II}(L_3)\}$$

and

$$\Delta E_{III/II}(L') = (1/3)\{E_{III/II}(L'_3) - E_{III/II}(L_3)\}.$$

Similarly, for the reversible half-wave potential of the oxidation step we have

$$E_{IV/III}(L''_n L'_{3-n}) = n\Delta E_{IV/III}(L'') + (3-n)\Delta E_{IV/III}(L') + E_{IV/III}(L_3) \quad (3)$$

with

$$\Delta E_{IV/III}(L'') = (1/3\{E_{IV/III}(L''_3) - E_{IV/III}(L_3)\}$$

and

$$\Delta E_{IV/III}(L') = (1/3)\{E_{IV/III}(L'_3) - E_{IV/III}(L_3)\}.$$

Here, we chose $[Ru^{III}(acac)_3]$ as the reference complex, i.e. $E_{IV/III}(L_3) = +0.633$ V and $E_{III/II}(L_3) = -1.138$ V (versus Ag/0.1 mol dm^{-3} $AgClO_4$–acetonitrile) (see Table 5). The values of $\Delta E_{IV/III}(L')$ and $\Delta E_{III/II}(L')$ for several kinds of L′ are presented in Table 6. The $E^r_{1/2}$ values of some mixed-ligand complexes are then calculated by means of eqns. (2) and (3) and given in Table 7 together with the observed values. These values agree with each other within 35 mV except in the case of the Ru^{III}/Ru^{II} couple for $[Ru(dpm)_2(hfac)]$.

Recently, Haga *et al.* [38] presented a set of ligand parameters, P_L, of some bidentate ligands on the basis of similar linear relationships observed in the cases of the oxidation of $[Ru^{II}(bpy)_{3-n}L_n]$ (L = polypyridine or β-diketonate). It should be noted that their ligand parameters apply to the Ru^{III}/Ru^{II} couples and a different set of parameters must be used for the Ru^{IV}/Ru^{III} couples, as is readily shown by the difference between $\Delta E_{IV/III}(L')$ and $\Delta E_{III/II}(L')$ values (Table 6).

TABLE 6. Potential shift per one ligand referred to $[Ru(acac)_3]$ in 0.1 mol dm^{-3} TEAP–acetonitrile at 25 °C[a]

L′	$\Delta E_{IV/III}(L')$ (V)	$\Delta E_{III/II}(L')$ (V)
$hfac^-$	0.404[c]	0.499
$tfpb^-$	0.216	0.269
$tfac^-$ [b]	0.224	0.229
$bzac^-$ [b]	0.008	0.041
dpm^-	−0.059	−0.101
$mClma^-$ [b]	0.057	0.107
$mIma^-$ [b]	0.032	0.100

[a]Reference value, $E_{IV/III}(acac_3) = 0.633$ V and $E_{III/II}(acac_3) = -1.138$ V. [b]$tfac^-$ = 1,1,1-trifluoro-2,4-pentanedionate ion; $bzac^-$ = 1-phenyl-1,3-butanedionate ion; mClma = 3-chloro-2,4-pentanedionate ion; mIma = 3-iodo-2,4-pentanedionate ion. The values for these ligands were calculated from Endo's data [37]. [c]Estimated from Fig. 4.

Supplementary Material

Lists of final atomic coordinates, thermal parameters and structure factors may be obtained from the authors (correspondence should be made to G.P.S.).

Acknowledgements

The authors thank Professor Akira Ouchi of the University of Tokyo and Associate Professor Mamoru Shimoi of Tohoku University for the X-ray diffraction measurements and for their helpful discussions. They also thank Dr Hirotaka Nagao, Sophia University, for his help with the refinement of the X-ray analysis.

TABLE 7. Comparison between calculated and observed half-wave potentials[a] of mixed-ligand β-diketonatoruthenium complexes

Complex	$E^r_{1/2}(Ru^{IV}/Ru^{III})$		$E^r_{1/2}(Ru^{III}/Ru^{II})$	
	Calc.	Obs.	Calc.	Obs.
$[Ru(acac)(tfpb)_2]$ (2)	1.065	1.058 1.055 1.054	−0.600	−0.577 −0.586 −0.586
$[Ru(acac)_2(tfpb)]$ (3)	0.849	0.838	−0.869	−0.847
$[Ru(acac)_2(hfac)]$ (5)	1.037	1.047	−0.639	−0.605
$K[Ru(acac)(hfac)_2]$ (6)	1.441		−0.140	−0.14
$[Ru(dpm)_2(hfac)]$ (7)	0.919	0.910	−0.841	−0.763
$[Ru(acac)_2(mClma)]$	0.690	0.680[b]	−1.031	−1.03[b]
$[Ru(acac)(dpm)_2]$	0.515	0.519[c]	−1.340	−1.320[c]
$[Ru(dpm)_2(mIma)]$	0.547	0.580[c]	−1.240	−1.206[c]

[a]Against Ag|0.1 mol dm^{-3} $AgClO_4$–acetonitrile 25 °C. [b]From refs. 18 and 37. [c]From ref. 39.

References

1 (a) Y. Hoshino, Y. Yukawa, A. Endo, K. Shimizu and G. P. Satô, *Chem. Lett.*, (1987) 845; (b) Y. Hoshino, A. Endo, K. Shimizu and G. P. Satô, *J. Electroanal. Chem., 246* (1988) 225.
2 Y. Hoshino, *Doctoral Thesis*, Sophia University, Tokyo, Japan, 1988.
3 R. A. Palmer, R. C. Fay and T. S. Piper, *Inorg. Chem., 3* (1964) 875.
4 T. J. Pinnavaia and S. O. Nweke, *Inorg. Chem., 8* (1969) 639.
5 T. J. Pinnavaia, J. M. Sebeson, II and D. A. Case, *Inorg. Chem., 8* (1969) 644.
6 D. A. Case and T. J. Pinnavaia, *Inorg. Chem., 10* (1971) 482.
7 J. P. Collman, R. L. Marshall and W. L. Young(III), *Chem. Ind.*, (1962) 1380.
8 R. E. Sievers and K. C. Brooks, *Int. J. Mass Spectrom. Ion. Phys., 47* (1983) 527.
9 J. Saar, D. E. Smith and M. Cais, *J. Am. Chem. Soc., 107* (1985) 6807.
10 G. S. Patterson and R. H. Holm, *Inorg. Chem., 11* (1972) 2285.
11 R. Grobelny, B. Jezowska-Trzebiatowska and W. Wojciechowski, *J. Inorg. Nuc. Chem., 28* (1966) 2715.
12 G. W. Everett, Jr. and R. M. King, *Inorg. Chem., 11* (1972) 2041.
13 A. Endo, *Bull. Chem. Soc. Jpn., 56* (1983) 2733.
14 N. A. Lewis and B. K. P. Sishta, *J. Chem. Soc., Chem. Commun.*, (1984) 1428.
15 Y. Takeuchi, A. Endo, K. Shimizu and G. P. Satô, *J. Electroanal. Chem., 185* (1985) 185.
16 A. Endo, K. Shimizu and G. P. Satô, *Chem. Lett.* (1985) 581.
17 Y. Satsu, A. Endo, K. Shimizu, G. P. Satô, K. Ono, I. Watanabe and S. Ikeda, *Chem. Lett.*, (1986) 585.
18 A. Endo, Y. Hoshino, K. Hirakata, Y. Takeuchi, K. Shimizu, Y. Furushima, H. Ikeuchi and G. P. Satô, *Bull. Chem. Soc. Jpn., 62* (1989) 709.
19 S. Aynetchi, P. B. Hitchcock, E. A. Seddon, K. R. Seddon, Y. Z. Yousif, J. A. Zora and K. Stuckey, *Inorg. Chim. Acta, 113* (1986) L7.
20 A. Endo, M. Kajitani, M. Mukaida, K. Shimizu and G. P. Satô, *Inorg. Chim. Acta, 150* (1988) 25.
21 A. Endo, K. Shimizu, G. P. Satô and M. Mukaida, *Chem. Lett.*, (1984) 437.
22 T. Sakurai (ed.), *The Universal Crystallographic Computation Program System (UNICS)*, Crystallographic Society of Japan, Tokyo, 1967.
23 *International Tables for X-Ray Crystallography*, Vol. IV, Kynoch Press, Birmingham, U.K., 1974.
24 T. Kobayashi, H. Nishina, K. Shimizu and G. P. Satô, *Chem. Lett.*, (1988) 1137.
25 D. R. Eaton, *J. Am. Chem. Soc., 87* (1965) 3097.
26 H. Kobayashi, H. Matsuzawa, Y. Kaizu and A. Ichida, *Inorg. Chem., 26* (1987) 4318.
27 D. R. Eaton, A. D. Josey, W. D. Phillips and R. E. Benson, *J. Chem. Phys., 37* (1962) 347.
28 D. R. Eaton, W. R. McClellan and J. F. Weiher, *Inorg. Chem., 7* (1968) 2040.
29 K. S. Hagen, D. W. Stephan and R. H. Holm, *Inorg. Chem., 21* (1982) 3928.
30 R. H. Holm and F. A. Cotton, *J. Am. Chem. Soc., 80* (1958) 5658.
31 R. C. Fay and T. S. Piper, *J. Am. Chem. Soc., 85* (1963) 500.
32 G. K.-J. Chao, R. L. Sime and R. J. Sime, *Acta Crystallogr., Sect. B, 29* (1973) 2845.
33 H. Matsuzawa, Y. Ohashi, Y. Kaizu and H. Kobayashi, *Inorg. Chem., 27* (1988) 2981.
34 J. G. Leipoldt, S. S. Basson, G. J. Lamprecht, L. D. C. Bok and J. J. J. Schlebusch, *Inorg. Chim. Acta, 40* (1980) 43.
35 A. Navaza, C. D. Rango and P. Chappin, *Acta Crystallogr., Sect. B, 36* (1980) 696.
36 Y. Satsu, A. Endo, K. Shimizu, G. P. Satô, H. Matsuzawa, Y. Kaizu and H. Kobayashi, *52nd Ann. Meet. Chemical Society of Japan, Kyoto, 1986*, 4K05.
37 A. Endo, *Doctoral Thesis*, Sophia, University, Tokyo, Japan, 1986.
38 M. Haga, T. Matsumura-Inoue, K. Shimizu and G. P. Satô, *J. Chem. Soc., Dalton Trans.*, (1989) 371.
39 Y. Kasahara, Y. Hoshino, K. Shimizu and G. P. Satô, unpublished work.
40 G. W. Everett, Jr. and R. R. Horn, *J. Am. Chem. Soc., 96* (1974) 2087.